UNDERSTANDING THE SPATIAL DISTRIBUTION OF SNOW WATER EQUIVALENT AND SUBSEQUENT SNOWMELT RUNOFF PATTERN OF PAIRED BASINS IN SOUTHWEST MONTANA

Jason Welz[1], Jordy Hendrikx[1], Stuart Challender[2], and Paul Stoy[3]

ABSTRACT

This paper presents the initial results of a research project with the primary goal of investigating the hydrologic role of avalanche activity alongside the physiographic variables (i.e. elevation, slope, aspect, wind shelter/exposure, landcover, and solar radiation) that the snow hydrology community widely consider to be the dominant controls on the spatial distribution of snow water equivalent (SWE) and subsequent snowmelt runoff in alpine basins. An extensive field campaign was conducted in two adjacent alpine basins in southwest Montana from January 31 to August 21, 2013, consisting of three survey periods to capture snowpack metrics during the phases of (1) accumulation; (2) peak SWE, and (3) ablation/snowmelt runoff. During each period, the same stratified random sampling methods were used to measure snow depth and SWE at transects along elevation contours. Transects were spatially distributed with the goal of acquiring a representative sample of the aforementioned physiographic variables as well as the components of avalanche paths. After quantifying the contribution of each of these variables to the distribution of SWE, we will also consider their impact on the timing and magnitude of snowmelt runoff. This will be determined by correlation to stream discharge measurements that were collected throughout the 2012-2013 water year. The initial results are discussed as are the future steps. (KEYWORDS: snow water equivalent, mountain hydrology, avalanche, snowmelt, runoff)

INTRODUCTION & BACKGROUND

The combined hydroclimatology and topography of the U.S. Intermountain West cause the majority of watersheds in the region to be dominated by snowmelt runoff (Cayan, 1996; Serreze et al., 1999). The temporal pattern of snowmelt is vital to the functioning of the semi-arid ecosystems in this region, and to the utilitarian needs of the human infrastructure. As a result, operational forecasting must consider the factors that influence the magnitude and timing of snowmelt runoff in order to harness and allocate water resources appropriately. Consequently, research in snow hydrology has long focused on how to accurately determine the distribution of snow water equivalent (SWE) over landscapes of different scales and degrees of spatial heterogeneity to use as a metric for subsequent snowmelt runoff. In alpine catchments, depending on the scale and climate, the majority of previous investigations have concluded that some combination of the physiographic variables of: elevation, slope, aspect, solar radiation, landcover, and wind shelter/exposure, are dominant in explaining the spatial pattern of SWE (Elder et al., 1991, 1998; Luce et al., 1998; Erickson et al., 2005; Harshburger et al., 2010; Clark et al., 2011). Some studies have mentioned avalanche activity as also having a contribution, but only a few have given this variable full consideration (Iveronova et al., 1965; de Scally and Gardner, 1988; de Scally, 1996). The goal of this current study is to expand upon, and take a comprehensive look at the effect of all of the variables, including avalanche activity, which may have an influence on the distribution of SWE in paired alpine basins in southwest Montana.

Avalanche activity can play an important role in this system by increasing or decreasing the melt rate that occurs from the redistribution and metamorphosis of the undisturbed snow cover. While research investigating this process has shown evidence in both directions, the majority of the literature points towards avalanche activity having the hydrologic role of extending the period of snowmelt (Iveronova et al., 1965; de Scally and Gardner, 1988). This phenomenon was further explored by de Scally (1996) in the Cascade Range of British Columbia by comparing the resultant runoff of two adjacent basins: one avalanche-prone and one relatively avalanche-free (control basin). The results of the data collected for three consecutive spring/summer runoff periods showed that 16-35% of the difference in unit area discharge between the basins was accounted for by the presence of snow in the avalanche-prone basin after all snow had disappeared in the control basin. While this was attributed to the persistence of large avalanche deposits in the avalanche basin, it was also stated that the majority of this difference

Paper presented Western Snow Conference 2014
[1]Jason Welz and Jordy Hendrikx, Snow and Avalanche Laboratory, Department of Earth Sciences, Montana State University- Bozeman, jason.welz@msu.montana.edu
[2]Stuart Challender, Department of Earth Sciences, Montana State University- Bozeman
[3]Paul Stoy, Department of Land Resources and Environmental Science, Montana State University- Bozeman

was possibly due to far greater losses in evapotranspiration that occur in the heavily forested control basin. Other topographic differences between the basins were mentioned as possibilities for the difference in snowmelt attenuation. These concerns highlighted the difference in the two basins with respect to physiographic features. An additional concern was the amount that each basin's snowmelt can be affected by heavy rain during the late spring/early summer period in a maritime climate.

This work continues to explore the results of the previous work but as it relates to mountainous regions of the U.S. Intermountain West. To accomplish this, the paired basin comparison design as used by de Scally (1996) to examine the role of avalanche activity, as well as a multitude of previous hydrologic projects, was used as the general framework. However, a conscious attempt was made to select a study area that would avoid the large differences in terrain variables which caused uncertainty in the results from de Scally (1996). While the study area of de Scally (1996) involved avalanche-prone and control basins of 5.0 and 11.8 km^2 respectively, the current research examines smaller basins with areas of 1.38 and 1.62 km^2. The significantly smaller scale of these basins allowed for finer sampling resolution of the snow cover distribution, which reduces the uncertainty of analyses. In addition, the ease of access to the current study area enabled frequent visits for acquiring a large and robust dataset. The paired basins were chosen to be as similar as possible with respect to area and elevation range with the assumption that snowfall accumulation and total snow water equivalent would be roughly the same after accounting for wind redistribution, solar radiation input, and avalanche activity. A particular effort was made to select sites with similar tree and vegetation coverage to avoid the variable that created the most uncertainty for the previous research. This research was performed in an intermountain snow climate with substantially different weather patterns, snow accumulation, and avalanche dynamics than the study site of de Scally (1996). This will likely eliminate some of the uncertainty in the resulting runoff brought about by melt season rain, as the intermountain west generally experiences far less of this pattern than the maritime region (Cayan, 1996). Furthermore, a study in this snow climate will present new information as to how the avalanche dynamics of this particular region translate to the possible effects on the timing and magnitude of snowmelt runoff.

STUDY AREA

The area selected for this research comprises paired alpine basins on the east slopes of Cedar Mountain (approximate center: N 45° 14' 3" W 111° 29' 42") in the Madison Range near Big Sky in southwest Montana (Figure 1). The more avalanche-prone basin (Basin A) has an area of 1.38 km^2 rising from 2721 to 3251 m, with predominantly east to northeast facing terrain forming the headwaters of the South Fork of the West Fork of the Gallatin River. Directly south, the control basin (Basin B) has an area of 1.62 km^2 ranging from 2645 to 3253 m. with generally east to southeast facing terrain. Average slopes are 24.2° and 22.5° for Basin A and B, respectively, and 32% of the area in each basin is considered avalanche terrain (slope > 30°). Both basins are undeveloped and exhibit land cover typical of an alpine environment in this region, with sparse ground cover vegetation covering the majority of the area and riparian shrubs limited to stream channels. Conservative estimation of tree cover, from satellite imagery in a GIS, is approximately 7% for Basin A and 19% for Basin B. Tree cover consists entirely of evergreen species.

This area of southwest Montana has been generally classified as having an inter-mountain snow climate (Mock and Birkeland, 2000). However, lying on the northern end of the intermountain zone at high elevation, cold average temperatures result in the snowpack of the Big Sky area to trend more towards a continental regime (Mock and Birkeland, 2000). The 20-year (1991-2010), October 1 - May 10 averages for precipitation (538 mm) and snow water equivalent (480 mm) from the NRCS Lone Mountain SNOTEL at 2707 m (approximately 6.5 km from the study site), also indicate this area receives less precipitation than some intermountain ranges to the south such as the Tetons and Wasatch. This cold and relatively drier climatic pattern has an important influence on the magnitude of snow redistributed by wind, as well as potential avalanche activity that can occur due to persistent weaknesses in the typical stratigraphy of this snowpack.

The primary attributes assumed to separate Basin A and B into avalanche-prone and control are their dominant topographic features and distribution of aspect. This applies to the steep, north/northeast facing headwall of Basin A for which 100% of the slope is greater than 30°. This combination of slope and aspect creates more potential for wind loading of snow, causing frequent sloughing and the occasional release of slab avalanches. In comparison, the east/southeast facing headwall of Basin B has less than 50% of its terrain with slopes greater than

30°. It is thought to have less potential for avalanche activity due to more wind scour than deposition and a less expansive avalanche start zone. Consideration of these variables is further addressed in the methods section.

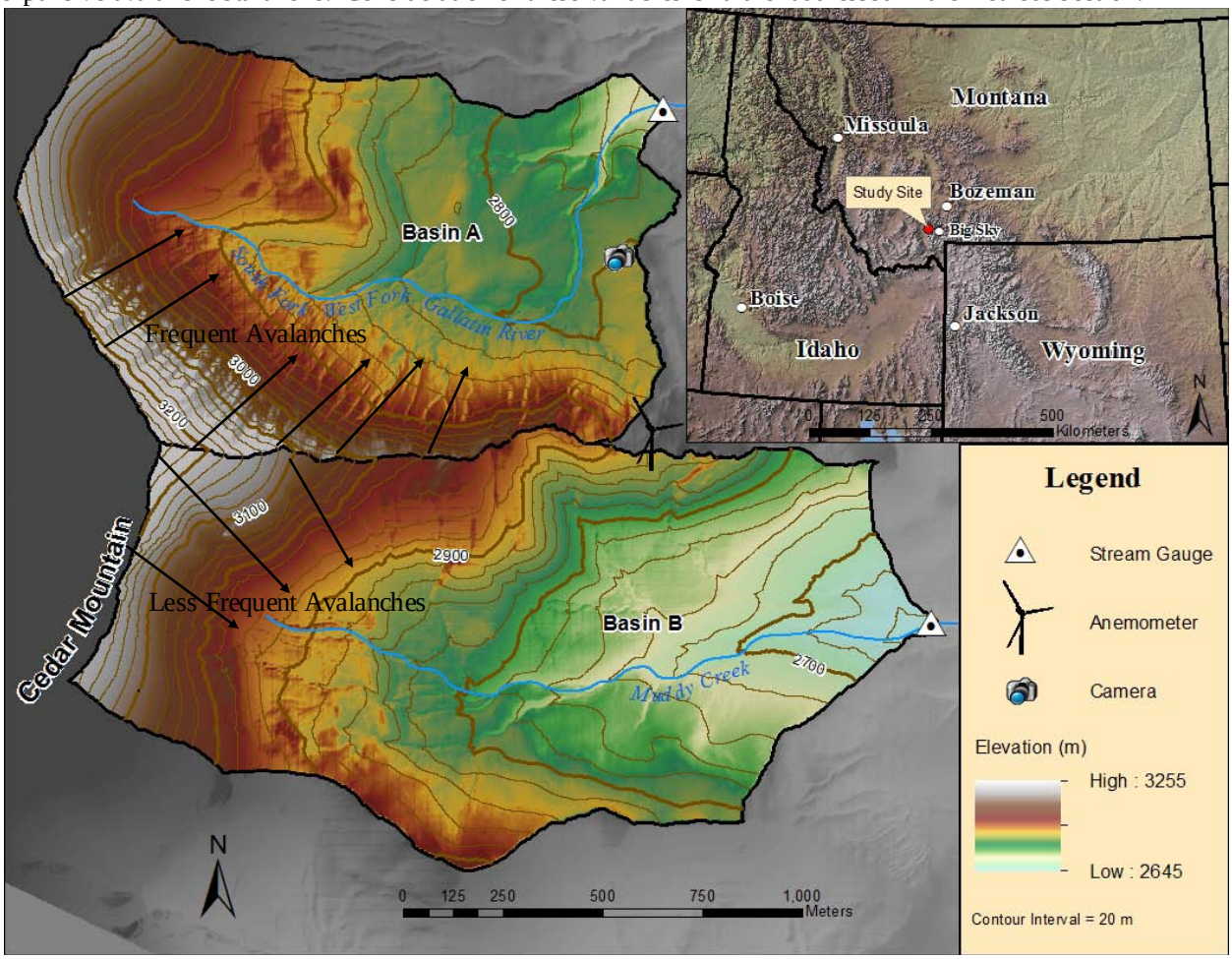

Figure 1. Map of the study site showing the distribution of elevation, aspect, and topographic features associated with avalanche activity.

METHODS

Classification of Strata by Physiographic Variables

Snowpack data collection employed a semi-random, stratified sampling strategy based on the goal of capturing a representative sample from each basin's distribution of the physiographic variables (i.e. elevation, slope, aspect, solar radiation, wind shelter/exposure, and avalanche activity). Elevation, slope, and aspect were modeled with a 1 m LiDAR DEM in ESRI ArcGIS ArcMap10.2, while a 10 m DEM was utilized for solar radiation to decrease the substantial computation time required for a six month period. Elevation was reclassified into 10 equal interval (approximately 61 m) strata to span the full range of the study area, 2645-3255 m. In reclassifying slope, its relationship to solar radiation intensity, wind shelter/exposure, and avalanche activity was considered. Hence, lower angle areas where solar intensity and wind redistribution are less influential were lumped into a 0-15° strata. Conversely, very steep areas that tend to be largely snow-free due to the more profound effect of these variables, were categorized into 60-90°. For avalanche activity, the second lowest strata, 15-25°, was considered to span the upper limit of runout zones and lower limit of avalanche tracks. Seven, 5° strata spanning 25-60°, were used to classify the remaining terrain, not only to represent the range of over which approximately 98% of all dry-slab avalanches occur (McClung and Schaerer, 2006), but to capture the small scale topographic features affecting solar intensity/shading and wind redistribution. Due to the circular nature of aspect data, it was transformed into a variable of northness (Harshburger et al., 2010) by taking the cosine of degrees from north. This yielded surrogate values for aspect between -1 (due south) and +1 (due north) that were used in analysis. The area solar radiation calculation tool

in ESRI ArcGIS 10.2 was used to model the daily accumulated solar radiation in watt hours per square meter (WH/m^2) from November 1, 2012 to May 1, 2013. While the slope strata indirectly incorporates avalanche activity, another strata was created to simplify the correlation of avalanche zone with the distribution of SWE. This involved classifying slope into strata of the typical angle ranges of avalanches zones (McClung and Schaerer, 2006): runout (<15°), track (15-30°), and start (<30°). A method to quantify the effect of wind redistribution is still in progress, but will likely be a simplified utilization of the upwind slope parameter (*Sx*) developed by Winstral et al. (2002) as an index of wind sheltering and exposure.

Snow Sampling Strategy

Once the physiographic strata were determined, a field sampling strategy was adopted by incorporating aspects of similar studies aimed at sampling SWE (e.g. Elder et al., 1998; Clark et al., 2011) and modifying them to match the scale triplet (spacing, extent, support, after Bloschl (1999)) considerations particular to the study area. While this strategy evolved during the three periods of data collection for the 2013 field campaign: accumulation (January 31-April 11), peak SWE (April 30-May 10), and ablation (June 2-July 10), the same general methods, and scale triplet were maintained. Sampling involved the collection of snow depth and SWE measurements at points along transects following elevation contours (Figure 2). Transects ranged 150-450 m in length with points spaced 20-50 m apart. Snow depth was measured with a 320 cm avalanche probe at the center of every point, as well as 1 m from the center in each cardinal direction (N, E, S, W). The average of the five depths was considered the snow depth value for that point. SWE was measured with a Federal snow sampler at a minimum of two, randomly, pre-chosen points along each transect. SWE values were used to calculate average snow density within each transect, which was then used to interpolate SWE across the entire transect from the depths.

Automated instrumentation was also installed to supplement snowpack measurements with respect to avalanche activity and wind (Figure 1). As a qualitative documentation of avalanche occurrences, a digital SLR camera was installed facing the northeast headwall of Basin A, as it was expected to experience the most frequent activity. The camera collected photos hourly (08:30-16:30) from December 17 to August 19, 2013. In order to have a site specific record of wind to enhance the analysis of this variable, an anemometer (Windlog, RainWise Inc.) was installed at 2808 m on the ridge separating Basins A and B. It recorded average wind speed (m/s) and direction (resolution: 22.5 degrees) over 15 minute intervals from December 17 to March 9, 2013. Neither the camera or anemometer data will be presented in this paper.

Multiple Linear Regression

Stepwise multiple linear regression (MLR) was used for a preliminary determination of the explanatory significance of the five independent variables: elevation, slope, northness, solar radiation, and avalanche zone on the dependent variable: SWE, thereby obtaining the most parsimonious models. This analysis was performed with the statistical software *R*, using the *lm* (linear model) function and adding variables in a stepwise fashion with different combinations until the highest multiple R-squared value was achieved with the fewest number of independent variables. In addition to the R-squared value, we also use the metrics of residual standard error (RSE) and the Akaike Information Criterion (AIC) to assist in our optimal model selection. This analysis provides an initial indication of which independent variables may be most dominant in each basin, thus providing a direction for subsequent, more in depth analyses.

Binary Regression Trees

Previous investigations into the spatial distribution of SWE in montane catchments (e.g. Elder et al., 1998; Balk and Elder, 2000; Winstral et al., 2002) have employed binary regression tree methods to interpolate this snowpack metric across the landscape. Harshburger et al. (2010) notes that this method requires large amounts of data and is therefore more accurate for small catchments, so it was considered ideal for this current study. The general binary tree technique developed by Breiman et al. (1984) works by the successive partitioning (splitting) of independent variable values to reach a predicted dependent variable value (terminal node). For the current study, this analysis was accomplished in *R* using the *rpart* function with the physiographic variables as splitting criteria growing towards terminal nodes of SWE. Overfitting is common problem with this method, where a tree is created that is too complex (i.e. involves too many splits) thereby lowering its true classification accuracy. Consequently, pruning was performed in *R* using the *pfit* function to grow a tree of optimal size and hence, have the highest predictive power.

Stream Discharge Measurement

In order to obtain continuous measurements of stage, a HOBO water level logger (model U20: 0 to 9 m depth) was installed in the outlet stream of each basin (Figure 1) and recorded stream stage hourly from November 1 to August 21, 2013. Stream velocity was measured every two weeks from June 13 to August 21, 2013 with a Marsh-McBirney Model 2000 flowmeter and wading rod along a cross-section at the water level loggers to generate a ratings curve from which to estimate discharge. The stream discharge data will not be presented in this paper.

RESULTS

Snow Sampling Distribution

Snow depth and SWE observations were made during the following three periods (Table 1):

(1) Accumulation season: January 31; February 7, 19; March 7, 26; and April 4, 11
(2) Peak SWE: April 30; May 5-7, 9, and 10 (Figure 2)
(3) Ablation season: June 2-3, June 13-14, June 26-27, and July 10

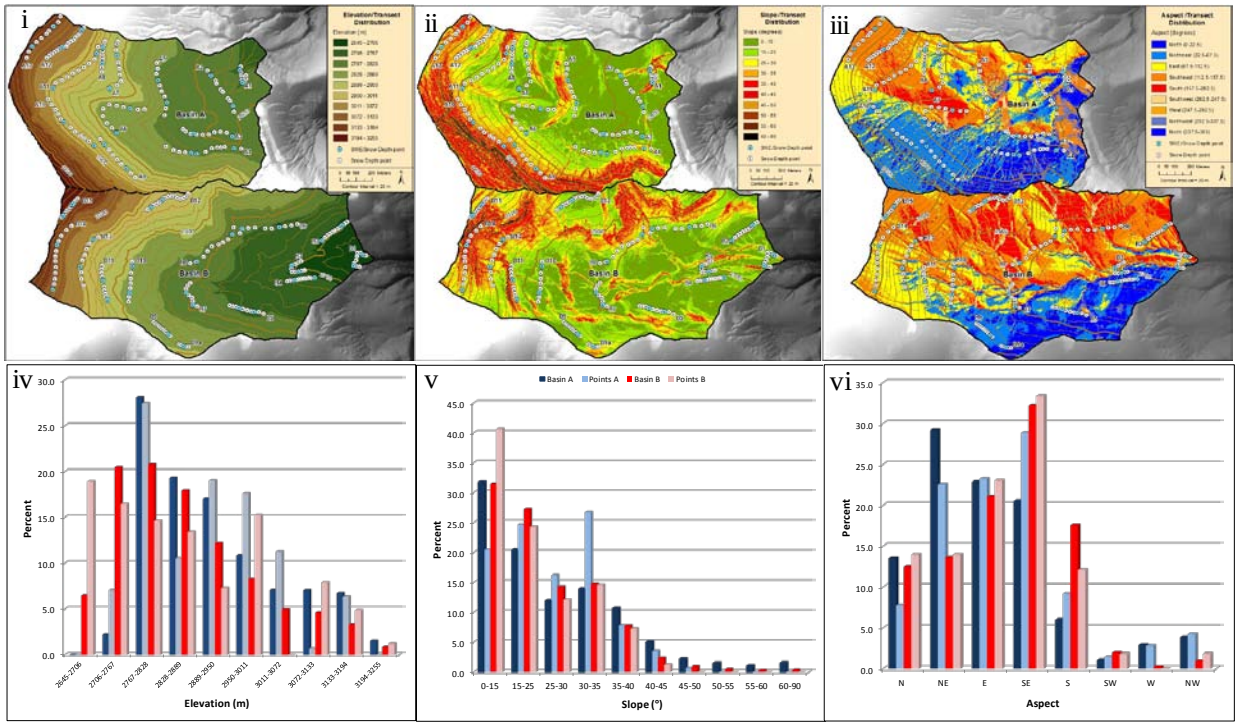

Figure 2. LiDAR (1 m) based maps of the study site showing the distribution of (i) elevation, (ii) slope, and (iii) aspect and the points sampled during peak SWE. The associated histograms show the actual physiographic variable distribution of (iv) elevation, (v) slope and (vi) aspect versus the sampling distribution for peak SWE.

Table 1. Summary of the snow sampling periods.

Sampling Period	Basin	Transects	Snow Depths	SWE msmts	Total Sample Points
Accumulation	A	9	109	10	170
	B	6	61	8	
Peak SWE	A	13	142	27	307
	B	15	165	30	
Ablation	A	12	127	25	255
	B	13	128	27	

Multiple Linear Regression

Because MLR analysis was carried out with all the independent (physiographic) variables with the notable exception of a wind shelter/exposure, it must be noted that these results are preliminary and may change given the anticipated importance of wind in distributing SWE at the study site. The results for the peak SWE period (Table 2) suggest that solar radiation, and the highly correlated variable of northness, as being the most dominant single parameter for Basin A, which is somewhat expected given the percentage of its area with a northerly aspect. This highlights the importance of shading as well as direct solar radiation for this basin. Adding avalanche zone, slope, or elevation as a second variable to solar radiation produces only a small increase in the R^2, decrease in the RSE and a small increase in the AIC, therefore suggesting that the addition of a second parameter does not sufficiently increase the explanatory power at the expense of model parsimony. The same can be observed for the models with three independent variables. In Basin B, northness also appears to be a dominant control, but solar is not, possibly indicating that the northness variable in this basin is more of a reflection of wind shelter given the predominantly southwest wind direction recorded at the onsite anemometer. This is also supported by the high rate of wind deposition that was observed at transect B13, which also produced some of the deepest snow depth and SWE measurements in the entire study site. Adding slope as a second variable to this model increases our explanatory power as indicated by the increase in R^2 from 0.1265 to 0.1987, as well as a decrease in RSE and AIC. Furthermore, there is another, smaller increase in R^2 from 0.1987 to 0.2210, and decrease in RSE and AIC with the inclusion of elevation as a third explanatory variable. Overall, these initial results suggest that SWE in both basins are being controlled by aspect (i.e. northness). It is unclear why solar radiation is a significant predictor (p-value: 2.2e-16) in Basin A, but not in Basin B (p-value: 0.0934) given the more dominantly north/northeast aspect of Basin A. This may be due to the effect of shading, rather than direct solar radiation. We anticipate that the explicit inclusion of wind in the models will help explain this and other questions brought up by these initial results.

Table 2. MLR results for the peak SWE sampling period listed in order of best fit (top) for each basin based on multiple R^2, residual standard error (RSE) and Akaike Information Criterion (AIC).

	Basin A				Basin B		
Model	**Multiple R^2**	**RSE**	**AIC**	**Model**	**Multiple R^2**	**RSE**	**AIC**
SWE~Solar	0.4938	255.8	1981.6	SWE~Northness	0.1265	322.7	2378.5
SWE~Northness	0.3895	281.0	2008.2	SWE~Slope	0.0632	334.2	2390.1
SWE~Elevation	0.1111	339.0	2061.6	SWE~Avalanche Zone	0.0484	336.8	2392.6
SWE~Avalanche Zone	0.0105	357.7	2076.8	SWE~Eastness	0.0235	341.1	2396.9
SWE~Slope	0.0102	357.8	2076.8	SWE~Solar	0.0172	342.3	2398.0
SWE~Eastness	0.0000	359.6	2078.3	SWE~Elevation	0.0036	344.6	2400.2
SWE~Solar + Northness	0.5163	251.0	1977.2	SWE~Northness + Slope	0.1987	310.0	2366.3
SWE~Solar + Avalanche Zone	0.4990	255.4	1982.2	SWE~Northness + Avalanche Zone	0.1759	314.4	2370.9
SWE~Solar + Slope	0.4987	255.5	1982.2	SWE~Northness + Elevation	0.1271	323.5	2380.4
SWE~Solar + Elevation	0.4943	256.6	1983.5	SWE~Slope + Elevation	0.1191	325.0	2381.9
SWE~Slope + Solar + Northness	0.5224	250.3	1977.4	SWE~Slope + Elevation + Northness	0.2210	306.6	2363.6
SWE~Aval Zone + Solar + Elevation	0.5029	255.4	1983.0	SWE~Slope + Solar + Northness	0.1992	310.9	2368.2
SWE~Slope + Solar + Elevation	0.5029	255.4	1983.0	SWE~Slope + Solar + Elevation	0.1316	323.7	2381.6

Binary Regression Trees

The initial binary regression tree for Basin A, like the MLR models, indicated the importance of northness, elevation, and slope, with splits occurring in that order (Figure 3). Pruning found it to be optimal with fewer splits and therefore, 6 terminal nodes instead of 8. For Basin B (Figure 3), splitting criteria also focused on northness, elevation, and slope with 10 terminal nodes, but the pruned model was optimized with 3 terminal nodes on just northness and elevation. Thus, aside from focusing on the importance of northness, the binary regression trees also indicated the importance of elevation, a variable that showed less explanatory value in the MLR. However, the variable of slope did reappear as an important variable, which was also used in the MLR for Basin B. Again, we anticipate that these results may change with the direct inclusion of a wind parameter.

FUTURE WORK

Further Statistical Analyses

For future analysis, we will add an explicit wind exposure/sheltering parameter, as we anticipate that this variable will be important in explaining the variability of SWE in our paired basins. We will also repeat the above analysis methods for the accumulation and ablation seasons, to examine if other variables become more/less important over time.

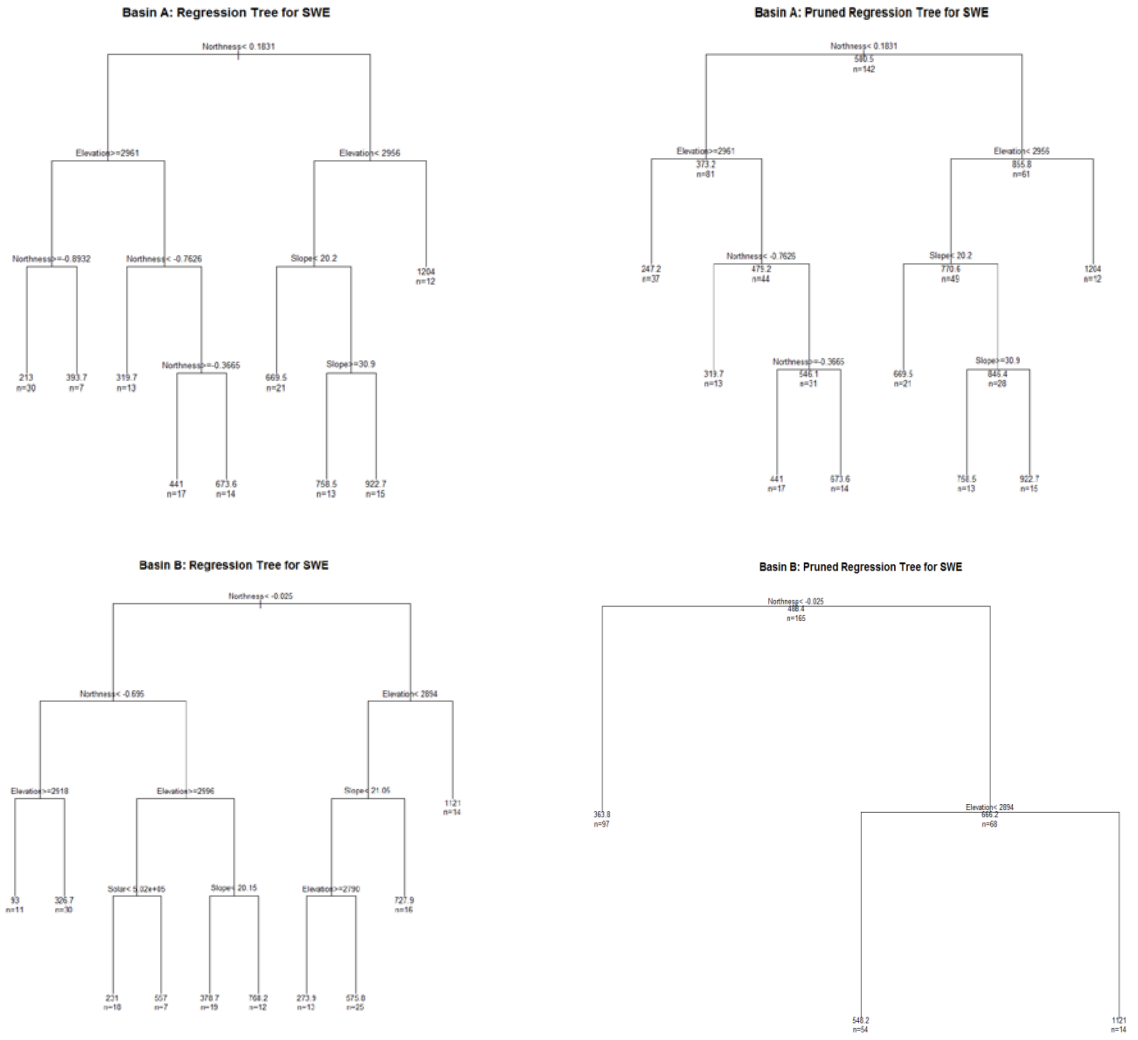

Figure 3. Initial and pruned binary regression trees for Basins A and B based on peak SWE sampling period data. Numbers at splits indicate the physiographic variable values of: northness (-1 to +1), elevation (m), slope (°), and solar radiation (cumulative WH/m^2). Terminal node values indicate predicted SWE (mm) along with the number of samples (n).

Stream Discharge Analyses

Cross-sectional flow velocity measurements made during each visit will be used to calculate stream discharge. A stage discharge relation graph will be plotted from the automated stream stage and manual stream discharge measurements in order to develop hydrographs for each basin. SWE data collected during the peak SWE period of field snow sampling will be analyzed with the hydrographs to investigate potential correlations between the variables affecting the spatial distribution of SWE and pattern of stream discharge.

CONCLUSIONS

The field snow sampling, automated wind and photography data, and initial analysis of this data has provided some insight on the dominant physiographic variables controlling the spatial distribution of SWE in each study basin. While substantial avalanche activity was expected to occur on the northeast headwall of Basin A, pre-analysis observations suggest that a relatively stable snowpack for the 2012-2013 season may have reduced the importance of this variable compared to other seasons. Our preliminary analysis suggests that the spatial distribution of snow depth and SWE can be best explained by solar radiation in Basin A and a combination of slope, elevation and northness in Basin B. Wind was not explicitly considered in this study, however it was certainly observed to be

a factor, especially in Basin B, where some of the deepest snow deposits were measured for the entire study site. These initial findings will continue to be tested with the statistical tools described, and the addition of an explicit wind parameter, with the goal of developing a reliable model to interpolate SWE across each basin. Ultimately, it is anticipated that this will provide direct correlation to what is observed in the resulting snowmelt runoff.

REFERENCES

Balk, B. and K. Elder. 2000. Combining binary decision tree and geostatistical methods to estimate snow distribution in a mountain watershed. Water Resources Research, 36: 13-26.

Blöschl, G. 1999. Scaling issues in snow hydrology, Hydrological Processes, 13: 2149-2175.

Breiman, L., J. H. Friedman, R. A. Olshen, and C. J. Stone. 1984. Classification and Regression Trees. Wadsworth, 358 pp.

Cayan, D.R. 1996. Interannual climate variability and snowpack in the western U.S. J. of Climatology 9: 928-948.

Clark, M.P., J. Hendrikx, A.G. Slater, D. Kavetski, B. Anderson, N.J. Cullen, T. Kerr, E.Ö. Hreinsson, and R.A. Woods. 2011. Representing the spatial variability of snow water equivalence and land surface models: a review, Water Resources Research, 47: W07539 1-23.

de Scally, F. A., and J. S. Gardner. 1988. The hydrological importance of avalanche snow, Kaghan Valley, Himalaya Mountains, Pakistan. International Snow Science Workshop, Whistler,B.C., Oct. 11-15, 1988.

de Scally, F.A. 1996. Avalanche snow melting and summer streamflow differences between high–elevation basins, Cascade Mountains, British Columbia, Canada. Arctic and Alpine Research, 28(1): 25–34.

Elder, K., J. Dozier, and J. Michaelsen. 1991. Snow Accumulation Distribution in an Alpine Watershed. Water Resources Research, 27(7): 1541-1552.

Elder, K., W. Rosenthal, and R.E. Davis. 1998. Estimating the spatial distribution of snow water equivalence in a montane watershed. Hydrological Processes, 12: 1793 – 1808.

Erickson, T.A., M.W. Williams, and A. Winstral. 2005. Persistence of topographic controls on the spatial distribution of snow in rugged mountain terrain, Colorado, United States, Water Resources Research, 41: 1-17.

Harshburger, B.J., K.S. Humes, V.P. Walden, T.R. Blandford, B.C. Moore and R.J. Dezzani. 2010. Spatial interpolation of snow water equivalency using surface observations and remotely sensed images of snow-covered area. Hydrological Processes. 24: 1285–1295

Iveronova, M. I. 1965. Le rôle hydrologique des avalanches. IASH, Proceedings International Symposium Scientific Aspects of Snow and Ice Avalanches, Davos, 73-77.

Luce, C., D. Tarboton, and K. Cooley. 1998. The influence of the spatial distribution of snowon basin-averaged snowmelt. Hydrological Processes, 12:1671–1683.

McClung, D. and P. Schaerer. 2006. The Avalanche Handbook. Seattle, WA: The Mountaineers.

Mock, C.J.and K.W. Birkeland. 2000. Snow Avalanche Climatology of the Western United States Mountain Ranges. Bull. Amererican Meteorological Society, 81, 2367–2392.

Serreze, M.C., M.P Clark, R.L. Armstrong, D.A. McGinnis, and R.S. Pulwarty. 1999. Characteristics of the western United States snowpack from snowpack telemetry (SNOTEL) data. Water Resources Research, 35: 2145 – 2160.

Winstral, A., K. Elder, and R.E. Davis. 2002. Spatial snow modeling of wind- redistributed snow using terrain–based parameters. Journal of Hydrometeorology, 3:524–538.